Thermal and Optical Study on the Frequency Dependence of an Atmospheric Microwave Argon Plasma Jet

Christoph Schopp, Nikolay Britun, Jan Voráč, Petr Synek, Rony Snyders, and Holger Heuermann, *Member, IEEE*

Abstract—This paper presents the frequency- and power-dependent thermal and spectral properties of a microwave argon plasma jet in the gigahertz range. These properties are determined at 1.3 GHz, 2.4 GHz, and 3.5 GHz for input powers from 2 W to 15 W and gas-flows from 1 to 4 $L\,m^{-1}$, including the influence of an argon/nitrogen mixture. These investigations are performed to determine the specific influence of the excitation frequency on the spectral properties of the plasma. The gas temperature is determined via the hydroxyl radical (OH) rotational band around 310 nm by fitting the simulated spectrum to the measurements. It is shown that high temperatures above 1350 K are generated inside the plasma for an input power of 10 W. At the same time, selective discharge 2-D mapping is realized as a result of charge-coupled device (CCD) imaging through optical bandpass filters, corresponding to the OH, N_2, Ar, and H spectral emission lines. It is found that all the investigated species change their size proportional to the size of the plasma. Influence of nitrogen is investigated by generating an argon/nitrogen gas mixture. The nitrogen admixtures up to 2% are examined. These investigations are based on measurements of the N_2-band around 370 nm. A strong dependence of the discharge appearance on the nitrogen content is found.

Index Terms—Frequency dependence, optical emission spectroscopy (OES), plasma applications, plasma generation, plasma jet, plasma properties.

I. INTRODUCTION

MICROWAVE plasma jets have been in the focus of research for a long time in versatile areas of applications. The geometry and a comparison of a jet to other plasma sources are given in [1]. Typical applications range from material processing to medical purposes [2]–[5]. The input power is dependent on the application and ranges from several watts to the megawatts area. Plasmas generated at

Fig. 1. Top: Argon plasma jet at 2.4 GHz and 5 W. Bottom: cross-cut of the coaxial geometry directing the microwave power to the plasma. Outer diameter: 20 mm. Inner diameter: 16 mm. Length: 85 mm.

microwave frequencies are sustained by capacitive coupling of the power allowing configurations such as enclosure by quartz glass and electrode-less lamps [6].

A strong dependence on the spatial properties of a microwave argon plasma jet (Fig. 1), as well as an increase of the energy density at higher frequencies, has been shown in [7].

In this work, an optical study is performed via optical emission spectroscopy (OES) to determine the influence of the excitation frequency, power, gas flow, and gas mixture on single spectral lines of the plasma to optimize the plasma operation to the desired applications. The main goal of this work is the analysis, whether the spectral lines contribute equally to the global effects (spatial extension of the plasma, energy density distribution) and if changes are limited to a specific spectral area. Independence of the plasma properties to the frequency leads to higher adaptability of the jet properties (size and excitation frequency) to the specific applications. A microwave argon plasma jet operated at frequencies around 1.3 GHz, 2.4 GHz, and 3.5 GHz and power levels from 2 W to 15 W are utilized. The frequency dependence of the gas temperature and the spatial extension of the plasma in different spectral bands are investigated.

II. THEORETICAL BACKGROUND

The plasma is powered by electromagnetic waves in the gigahertz-range which are subject to the same laws as optical

waves. They are refracted upon propagating from one medium into another and upon changes of the dielectric properties. The microwave power at a defined reference plane is equal to the difference of the transmitted and reflected power. Further explanations of RF power measurements are given in [8].

During optical measurements, a conical or cylindrical region of the plasma is measured typically along the line of sight. From the obtained data, the relative density of emitters present in the emitting area can be extracted. Based on specific characteristics of the species, different characteristic plasma temperatures are pronounced (each one representing an excitation of a certain degree of freedom in the gas): rotational, T_{Rot}, vibrational T_{Vib}, and electron T_{El}.

The rotational and vibrational temperature T_{Rot} and T_{Vib} are calculated using *massiveOES* software package that fits the model spectral profile to the measured spectral data.

The model is constructed by finding all the rotational lines lying in the observed spectral region in the *massiveOES* database. For OH species, the database used information from [9]–[11]. The strength $\Phi_{u,l}$ of each line is given by

$$\Phi_{u,l} = n_u A_{u,l} \qquad (1)$$

where n_u is the relative population of the respective upper state and $A_{u,l}$ is the transition probability for the line in s^{-1}. In this case, the strength is proportional to the flux of photons originating from the respective transition. The relative population of each upper state is calculated under the assumption of the Boltzmann distribution which is given by the respective Boltzmann fraction. The rotational and vibrational temperatures are treated independently (for details see [12] and [13]).

The artificial spectrum is subsequently broadened by convolution with a Voigt profile, defined by Gaussian half-width at half-maximum (HWHM) G and the Lorentzian HWHM L. The broadening of each line in the spectrum is assumed to be equal. This approach can be used if the instrumental broadening of lines dominates, which is satisfied in our case.

The differences of measurement and simulation are then calculated at each point, and the sum of their squared values is minimized with respect to the fit parameters which were: constant background, starting wavelength, linear, and quadratic term for wavelength correction, the Gaussian broadening HWHM, the Lorentzian broadening HWHM, relative OH "intensity," rotational, and vibrational temperature.

The rotational temperature of OH(A) is considered to reflect the kinetic temperature of the gas in this particular case, even though it is known that rotational distribution of OH(A) spectra may seriously deviate from thermal equilibrium. The main reason for this deviation is the OH(A) lifetime reduction by electronic quenching. The quenching of OH(A) by argon atoms is extremely slow and practically does not reduce its natural lifetime. On the other hand, water vapor is a very efficient quencher. Bruggeman *et al.* [14] identified the amount of water vapor leading to serious deviations of OH(A) T_{Rot} from the kinetic temperature of the gas as 1000 ppm. In this experiment, no water has been intentionally added to the feed gas. We estimate the amount of water as an impurity to be well below 100 ppm, corresponding to OH(A) quenched lifetime of 500 ns. In these conditions, the rotational
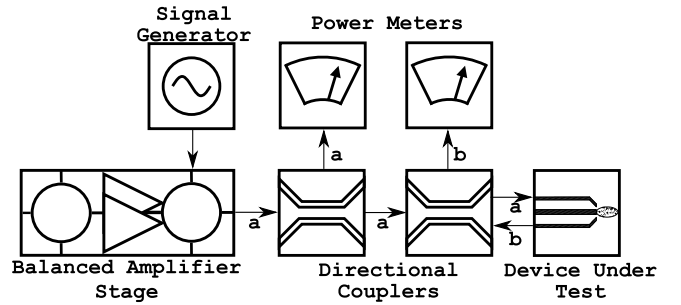
Fig. 2. Block diagram of the measuring set-up to operate the jet. Input power is created by a signal generator and an amplifier. (a) Transmitted and (b) reflected waves are monitored by two power meters.
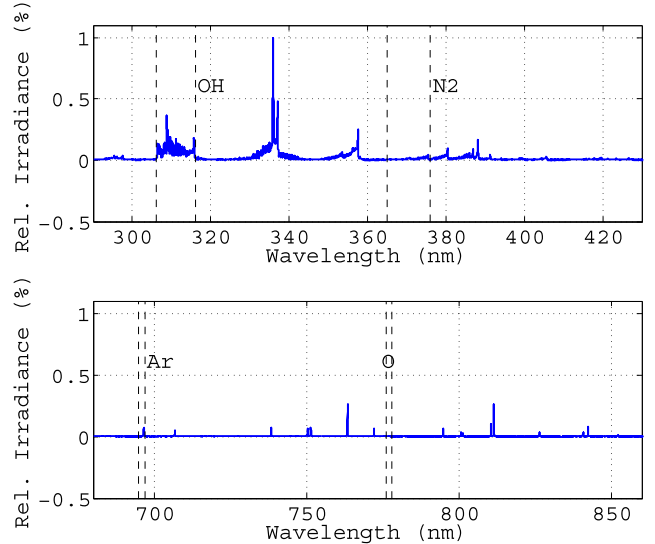
Fig. 3. OES spectra of the plasma jet from 290 nm to 860 nm. The area from 430 nm to 680 nm is omitted due to nonpronounced spectral lines. Key emission line areas are marked with the corresponding species.

temperature of OH(A) has been confirmed to agree with the kinetic temperature of the gas. In the case of this work, the rotational temperature is assumed to be equal to the gas temperature [15].

III. EXPERIMENTAL SETUP

The jet (also used in [7]) consists of a standard N-plug with an attached hollow cylinder topology. A coaxial network is formed by the cylinder and an inner conductor (length: 85 mm, diameter: 20 mm, inner diameter: 16 mm). In a coaxial network, the diameter ratio of the inner and outer conductor determines the wave impedance. To match the amplifier impedance to the electrical impedance of the plasma, different diameters, and lengths of the inner conductor are utilized. The power is supplied through the plug, as indicated in Fig. 1 (bottom).

In Fig. 2, the block diagram of the experimental setup to generate the high-frequency power is plotted. The combination of a Stanford Research SG384 signal generator and different amplifier setups (at 1.3 GHz by two balanced Mitsubishi RA18H1213G, at 2.4 GHz by an HHFT PlasMaster 100 W, and at 3.5 GHz by two balanced WiMax amplifier stages) provide the power. Two Narda 3022 bidirectional coaxial couplers monitor the transmitted and reflected wave using a
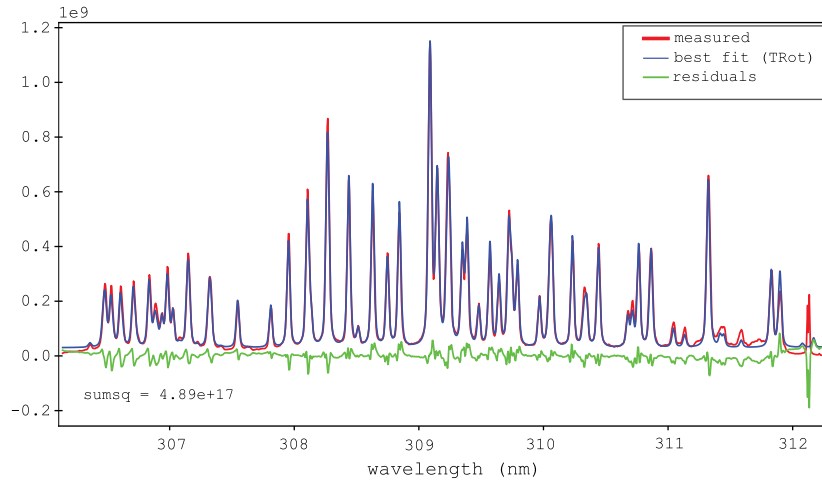
Fig. 4.   Measured and fit OH-band around 310 nm to determine the rotational temperature T_{Rot}. Residuals display the difference between the measured and the fit results. Spectra is captured at 2.4 GHz and 10 W using an optical bandpass filter.

Gigatronics 8543C power meter, an HP 8481 power sensor, and an HP 8481D power sensor. The power at the reference plane, located at the plug of the jet, is equal to the power coupled into the plasma due to the negligible transmission losses of the jet.[1]

The optical properties of the plasma are measured via OES. It is a noninvasive method analyzing the spectrum of an emitting source at certain wavelengths. The measurements are performed using an Andor SR-750 monochromator with an Andor iStar 740 series intensified charge-coupled device (ICCD) camera for the spectra acquisition and the ICCD camera with a Nikon AF 50 mm f/1.4D lens for OES imaging. The spectrometer resolution is equal to about 30 pm for the spectral measurements, for which a 2400-gpmm grating is used. Optical bandpass filters with a bandwidth of 10 nm are utilized for the measurements of the significant spectral bands.

The amount of argon is set by a gas flowmeter. For the mixture with nitrogen, an additional gas flowmeter with adjusted flow value is utilized.

IV. MEASUREMENT RESULTS

The frequency- and power-dependent analysis of the measurement results are split into two parts. First, the results of the temperature determination are presented by fitting the 310-nm OH-band to the measured rotational spectra. It is followed by an investigation on the dependence of the spatial and optical properties of different bands on different parameters.

A. Measurement Method Description

In Fig. 3, the OES spectra corresponding to the 290–430-nm and the 680–860-nm ranges are plotted. All omitted areas do not contain any pronounced spectral lines. As can be seen from the marks in the spectrum, the analysis of the emission lines (OH, N_2, Ar, and O) is presented in this paper.

B. Temperature Fitting Using Hydroxyl Emission

Fig. 4 displays the comparison of the measured spectra from 306 nm to 312 nm along with the fit result for the rotational temperature T_{Rot}. This spectrum is recorded at 2.4 GHz and 10 W. The difference (residuals) of the measurement to the fitting is plotted with a maximum absolute value of 0.2×10^9 and a mean relative error of about 3%. As mentioned above, the accumulated measuring error is about 5% resulting in a combined relative error of 8% for the determination of the temperature.

In Fig. 5, the determined rotational temperature at 1.3 GHz, 2.4 GHz, and 3.5 GHz from 5 W to 15 W are presented. At 1.3 GHz and 15 W, the maximum temperature of 1350 K is attained. At the lower gas flow, a nonproportionality of the temperature to the power is visible in contrast to a proportionality at the higher gas flow of 4 Lm^{-1}. Higher temperatures are measured for the lower gas flows with a mean reduction of about 100 K at 4 Lm^{-1}. This suggests a cool down by a higher convection cooling.

In [7], it is observed that both size and emission intensity decrease over frequency. The emission intensity of the plasma area is normalized to its spatial extension resulting in an almost constant ratio. Therefore, the proportionality of the energy density and frequency is assumed. It is supported by [16], where an increase of the electron density at higher frequencies is presented. The increase of the electron density may lead to a higher overall gas temperature due to an increase of the particle collisions.

A direct connection between the gas temperature and the frequency cannot be extracted from the measurements because of the increased temperature at the intermediate frequency of 2.4 GHz. This increase might be caused by a slight mismatch at this frequency, where more power was coupled into the plasma than measured.

C. Spectral Analysis

This section describes the individual influence of the frequency, power, gas flow, and gas composition on the apparent size of the plasma when observed through different spectral

---

[1]Losses vary from 0.1 dB at 1.3 GHz, over 0.16 dB at 2.4 GHz, to 0.13 dB at 3.5 GHz.
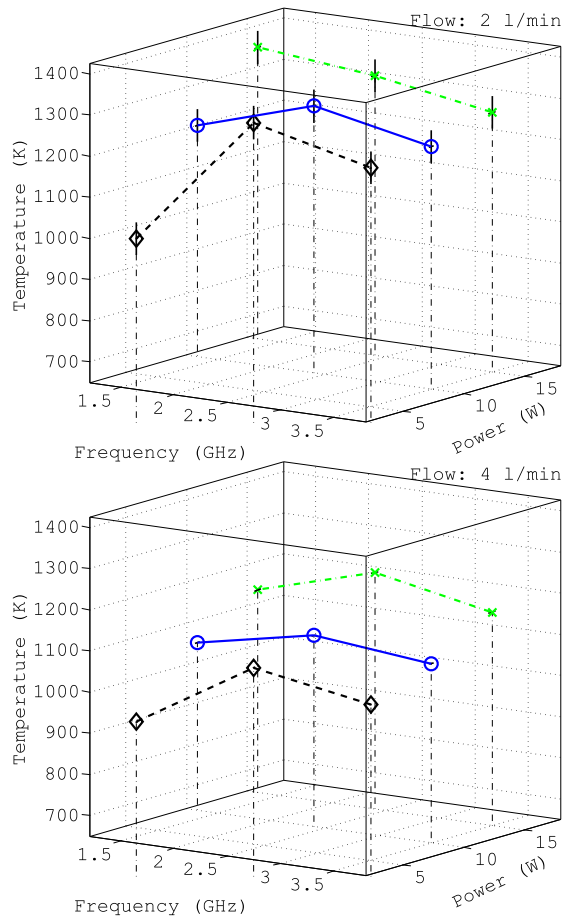
Fig. 5. Fit temperature from 1.3 to 3.5 GHz and powers from 5 to 15 W for argon gas flows of 2 and 4 Lm^{-1}. Measuring accuracy of the power is 5%.

filters. All images have been scaled to the same size for a direct visual comparison of the effects.

The plasma shapes at three microwave discharge frequencies and input power levels with a constant argon flow of 2 Lm^{-1} are illustrated in Fig. 6. The largest spatial extension is measured for 1.3 GHz and 15 W. The size of the plasma is proportional to the input power and inversely proportional to the frequency. It is assumed that the proportionality of the size and the frequency is caused among other things by two factors: the decrease of time in which the electric field accelerates the free charge carriers and the proportionality of the electron density to the frequency. All images exhibit a halo effect around the plasma with an inner core of higher light intensity. This effect has also been used in [17] to generate a more accurate 3-D finite element method-model for the simulation of the electrical plasma parameters.

A size comparison of an argon plasma for spectral bands around 310 nm (OH), 370 nm (N_2), 696 nm (Ar), and 777 nm is shown in Fig. 7. All images are recorded at an argon flow of 4 Lm^{-1}, a power of 10 W, at 1.3 GHz, 2.4 GHz, and 3.5 GHz. For all spectral lines, the mean measured changes in the size are proportional to the input power and inversely proportional to the frequency. The differences of the size shown in Fig. 7 are caused by instabilities from the gas flow.

A halo around the plasma is only visible for the OH-line around 310 nm (Fig. 8) and the O-line at 777 nm (Fig. 7).
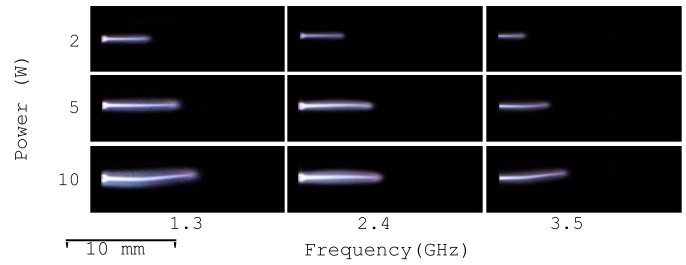
Fig. 6. Whole emission range shape of the plasma region as a function of discharge frequency at different frequencies and applied power. Argon flow is set to 2 Lm^{-1}.
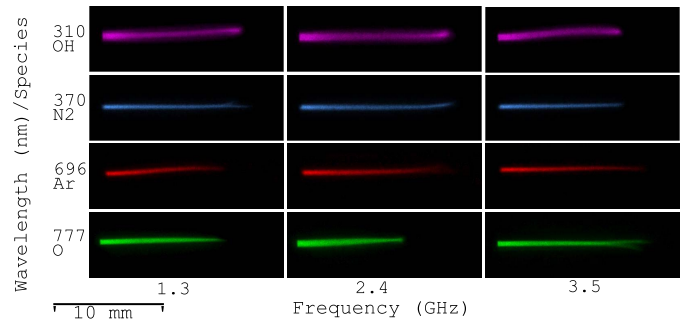
Fig. 7. Filtered plasma region shape as a function of the discharge frequency at different spectral emission lines (310, 370, 696, and 777 nm). Argon flow is set to 4 Lm^{-1}.
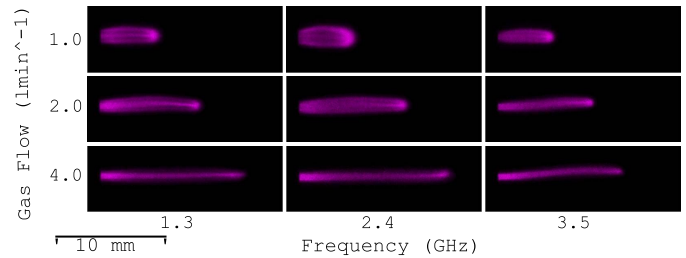
Fig. 8. Shape of the plasma region as a function of discharge frequency at different argon flows for the OH-band (filter at 310 nm) (left). Power is set to 10 W.
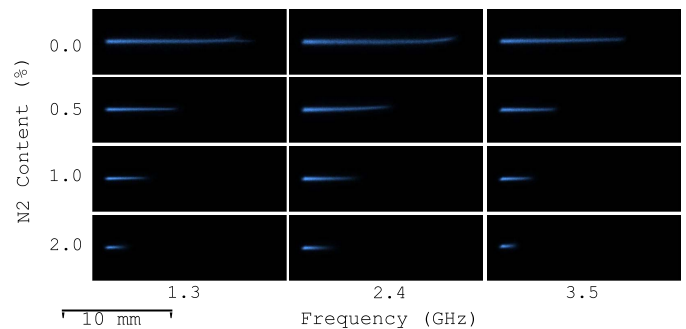
Fig. 9. Shape of the plasma as a function of discharge frequency at different nitrogen contents in the gas mixture. Filter for 370 nm is applied. Ar and N_2 flow is set to 4 Lm^{-1}.

All other spectral lines show the area of higher light output in the core of the plasma. This effect might be caused by oxygen and water particles diffusing from ambient air getting excited by collisions with active particles in the plasma plume. Minimal amounts of OH might be introduced by the gas supply system. The brightness of the halo shown in Fig. 6 suggests additional spectral emissions in the visible area. Some plasma plumes have a second ramification ("double tail") at their end, which is caused by the instabilities mentioned above.

The influence of the gas flow on the OH-band is presented in Fig. 8. Gas flow is swept from 1 L min^{-1} to 4 L min^{-1} and the frequency from 1.3 GHz to 3.5 GHz at 10 W. At a gas flow of 1 L m^{-1}, the horizontal size of the plasma is almost constant across all frequencies, while only the vertical size changes. Almost no inner core is visible at this gas flow. The horizontal size increases at 2 L m^{-1} for all frequencies, while the vertical size is decreased. An area of higher brightness is visible at the tail of the plume, which is connected via a slightly visible inner core. At 4 L m^{-1}, the horizontal size increases further while exhibiting the smallest vertical extent. The brightness of the plasma tail is decreased and the core of is more pronounced.

Fig. 9 displays the comparison of an argon/nitrogen mixture with a relative N_2 content from 0.0% to 2.0% at frequencies from 1.3 GHz to 3.5 GHz, an input power of 10 W and a combined gas flow of 4 L m^{-1}.

The size of the plasma is inversely proportional to the frequency and nitrogen amount, while the vertical extension is almost constant across all swept measurement parameters. The relative nitrogen amount is inversely proportional to the horizontal extent. Areas of higher light intensity are located at the tip of the electrode. This intensity increases with a decrease in the plasma size.

As mentioned above, the size reduction of the plasma in pure argon is mainly caused by the lower acceleration time of the free charge carriers at higher frequencies [7] and the generation of an increased electron density at higher frequencies [16]. For the gas mixtures, a size reduction at higher nitrogen amounts is observed. Nitrogen acts as an efficient quencher destroying the excited states present in the plasma. The amount of particle collisions increases with the gas flow, and therefore, the excited states are more reduced at higher concentrations of nitrogen. The size of the plasma is also reduced by the quenching effect at higher distances from the electrode.

It has been reported that a modulation superimposed on the input signal could facilitate mixing of the effluent gas with the ambient atmosphere, leading to similar effects as described above [18]. Therefore, further investigations are planned to characterize possible influences of a modulated signal on the frequency dependence of a plasma and the gas mixture.

All measured emission lines exhibit the same frequency-dependent behavior as the changes observed in [7]. The single spectral lines contribute equally to the size changes and energy density distribution. A halo surrounding the emission lines associated with oxygen is the only observed difference.

V. Conclusion

In this paper, the influence of frequency, power, gas flow, and gas composition on the thermal and optical properties of a microwave plasma have been investigated. Three frequency bands around 1.3 GHz, 2.4 GHz, and 3.5 GHz with power levels from 5 W to 15 W are utilized with a gas flow of up to 4 L m^{-1} are measured.

A maximum temperature of 1357 ± 40 K is determined by fitting the OH-band to the measurements. As expected the gas temperature is proportional to the input power but has a nonmonotonous connection to the frequency. An increase of the gas flow from 2 to 4 L min^{-1} lowers the mean temperature by about 150 K.

OES imaging for OH, N_2, Ar, and atomic oxygen excited states density mapping has shown that the changes of the spatial properties caused by any of the investigated parameters correspond proportionally for all optical bands. This means that none of the parameters has an influence on a specific spectral line. Therefore, these parameters can be utilized to adjust the plasma to the desired application without any disadvantages on the plasma properties. A plasma core is surrounded by a halo of lower brightness. This effect is observed in the bands associated with oxygen. These results are rather new and did not find any confirmation in the literature so far.

The gas mixture has a strong effect on the spatial extension of the plasma, which might be useful for adaptive control of the size, as well as improving the matching of the plasma impedance. A smaller size of the plasma at higher concentrations of nitrogen is measured. It is caused by efficient quenching of excited states of the plasma by the nitrogen atoms. To counteract the size change effect, a superimposed modulated signal could be used for further investigations.

In general, the results obtained in this work show that all spectral emission lines are proportional to the microwave frequency and that a nonmonotonous dependence of the temperature on the frequency exists. The proportional dependence on the frequency is important for applications since it offers a complete degree of freedom in the design of the jet. It is possible to adapt the frequency, and thus, the whole size of the jet to the application needs without any disadvantages to the plasma properties.

References

[1] A. Schutze, J. Y. Jeong, S. E. Babayan, J. Park, G. S. Selwyn, and R. F. Hicks, "The atmospheric-pressure plasma jet: A review and comparison to other plasma sources," *IEEE Trans. Plasma Sci.*, vol. 26, no. 6, pp. 1685–1694, Dec. 1998.

[2] H. Heuermann, S. Holtrup, A. Sadeghfam, M. Schmidt, R. Perkuhn, and T. Finger, "Various applications and background of 10–200W 2.45 GHz Microplasmas," in *IEEE MTT-S Int. Microw. Symp. Dig.*, Jun. 2012, pp. 1–3.

[3] A. I. Al-Shamma'a, S. R. Wylie, J. Lucas, and J. D. Yan, "Atmospheric microwave plasma jet for material processing," *IEEE Trans. Plasma Sci.*, vol. 30, no. 5, pp. 1863–1871, Oct. 2002.

[4] A. Stephan, H. Heuermann, and M. Prantner, "Cutting human tissue with novel atmospheric-pressure microwave plasma jet," in *Proc. 46th Eur. Microw. Conf.*, Oct. 2016, pp. 902–905.

[5] J. Choi, A.-A. H. Mohamed, S. K. Kang, K. C. Woo, K. T. Kim, and J. K. Lee, "900-MHz nonthermal atmospheric pressure plasma jet for biomedical applications," *Plasma Process. Polym.*, vol. 7, nos. 3–4, pp. 258–263, 2010.

[6] C. Schopp *et al.*, "Capacitively coupled high-pressure lamp using coaxial line networks," *IEEE Trans. Microw. Theory Techn.*, vol. 64, no. 10, pp. 3363–3368, Oct. 2016.

[7] C. Schopp, H. Heuermann, and M. Marso, "Multiphysical study of an atmospheric microwave argon plasma jet," *IEEE Trans. Plasma Sci.*, vol. 45, no. 6, pp. 932–937, Jun. 2017.

[8] A. A. Fantom, *Radio Frequency & Microwave Power Measurement*. London, U.K.: P. Peregrinus on behalf of the Institution of Electrical Engineers, 1990.

[9] J. Luque and D. R. Crosley, "Transition probabilities in the $A^2\Sigma^+–X^2\Pi_i$ electronic system of OH," *J. Chem. Phys.*, vol. 109, no. 2, pp. 439–448, Jun. 1998.

[10] K. L. Steffens, J. Luque, J. B. Jeffries, and D. R. Crosley, "Transition probabilities in OH $A^2\Sigma^+$–$X^2\Pi_i$: Bands with v'=2 and 3," *J. Chem. Phys.*, vol. 106, no. 15, pp. 6262–6267, Apr. 1997.

[11] L. R. Williams and D. R. Crosley, "Collisional vibrational energy transfer of OH ($A^2\Sigma^+$, v'=1)," *J. Chem. Phys.*, vol. 104, no. 17, pp. 6507–6514, May 1996.

[12] J. Vorác, P. Synek, V. Procházka, and T. Hoder, "State-by-state emission spectra fitting for non-equilibrium plasmas: OH spectra of surface barrier discharge at argon/water interface," *J. Phys. D: Appl. Phys.* vol. 50, no. 29, pp. 6507–6514, 1996.

[13] J. Vorác, P. Synek, L. Potocnáková, J. Hnilica, and V. Kudrle, "Batch processing of overlapping molecular spectra as a tool for spatio-temporal diagnostics of power modulated microwave plasma jet," *Plasma Sources Sci. Technol.*, vol. 26, no. 2, 2017, Art. no. 025010.

[14] P. Bruggeman, F. Iza, P. Guns, D. Lauwers, and M. G. Kong, "Electronic quenching of OH(A) by water in atmospheric pressure plasmas and its influence on the gas temperature determination by OH(A-X) emission," *Plasma Sources Sci. Technol.*, vol. 19, no. 1, Dec. 2009, Art. no. 015016.

[15] M. Bazavan, M. Teodorescu, and G. Dinescu, "Confirmation of OH as good thermometric species for gas temperature determination in an atmospheric pressure argon plasma jet," *Plasma Sources Sci. Technol.*, vol. 26, Jul. 2017, Art. no. 075001.

[16] P. Mérel, M. Tabbal, M. Chaker, M. Moisan, and A. Ricard, "Influence of the field frequency on the nitrogen atom yield in the remote plasma of an N_2 high frequency discharge," *Plasma Sources Sci. Technol.*, vol. 7, no. 4, p. 550, 1998.

[17] C. Schopp, "Characterization and multi-physical analysis of microwave plasma applications from 1.3 to 3.5 GHz," Ph.D. dissertation, Dept. Fac. Sci., Technol. Commun., Eng. Sci., Univ. Luxembourg, Luxembourg City, Luxembourg, 2018.

[18] J. Vorác, L. Potocnáková, P. Synek, J. Hnilica, and V. Kudrle, "Gas mixing enhanced by power modulations in atmospheric pressure microwave plasma jet," *Plasma Sources Sci. Technol.*, vol. 25, no. 2, Apr. 2016, Art. no. 025018.

Christoph Schopp received the Ph.D. degree in electrical engineering from the University of Luxembourg, Luxembourg, in 2018.

From 2008 to 2011, he was a Software Developer with Klafka & Hinz GmbH, Aachen, Germany. Since 2012, he has been with the Institute for Microwave of Microwave and Plasma Technology (IMP), Aachen University of Applied Sciences, Aachen. From 2012 to 2015, he was involved in electrodeless microwave-driven high-intensity discharge lamps. He is involved in the development of applications for microwave driven plasmas. He has authored or coauthored eight papers. His current research interests include 3-D-plasma printers, the frequency-dependence, and the modeling of microwave plasmas.

Nikolay Britun received the master's degree in quantum radiophysics from the Radiophysical Department, Kiev National University, Kiev, Ukraine, in 2002, and the Ph.D. degree in plasma diagnostics from Sungkyunkwan University, Seoul, South Korea, in 2008.

Since 2009, he has been a Researcher with the Laboratory Chimie des Interactions Plasma-Surface (Chemistry of Plasma-Surface Interaction), University of Mons, Mons, Belgium, collaborating with several schools over the World, such as the University of Lisbon, Lisbon, Portugal, Seoul National University, Seoul, Tokyo Metropolitan University, Hachioji, Japan, Chongqing University, Chongqing, China, Institute for Plasma Physics, Munich, Germany, and so on. He has authored or coauthored nearly 90 research articles and more than 100 contributions to numerous international conferences. His current research interests include optical characterization of the low-temperature and fusion plasmas, involving optical emission and absorption spectroscopy, and the laser-based methods for plasma diagnostics, especially gas conversion in low-temperature microwave discharges, characterization of magnetron sputtering discharges, laser-based diagnostics in the atmospheric plasma sources, and high-resolution spectroscopy in fusion plasma.

Jan Vorác received the Ph.D. degree in plasma physics from Masaryk University, Brno, Czech Republic, in 2014.

Since 2014, he has been a Researcher with Masaryk University, where he has been involved in spectroscopic diagnostics of plasma. He actively collaborates with INP Greifswald, Greifswald, Germany (fellowships in 2010, 2011, 2016, and 2017) and the University of Ghent, Ghent, Belgium, and the University of Mons, Mons, Belgium (fellowship in 2018). He has authored or coauthored 14 papers. He has coauthored MassiveOES open-source spectroscopic software. He holds two patents. His current research interests include optical emission spectroscopy, laser-aided plasma diagnostics (fluorescence and scattering measurements), and software development for spectroscopic data processing.

Petr Synek received the Ph.D. degree in plasma physics from the Department of Physical Electronics, Masaryk University, Brno, Czech Republic.

He was with the Central European Institute of Technology, Brno, where he was involved in the plasma diagnostics of the microwave discharges for nanomaterial synthesis and the characterization of nanomaterials like functional nanoparticles or carbon nanotubes. He has been with the Department of Physical Electronics, Masaryk University, where he has been involved in experimental data computer processing and statistical evaluation. He has authored or coauthored 27 papers. He has coauthored MassiveOES open-source spectroscopic software. His current research interests includes electrical and optical characterization of plasma discharges, with a focus on large data sample evaluation using computer-assisted methods.

Rony Snyders received the Ph.D. degree in chemistry from the University of Mons, Mons, Belgium, in 2004.

He was a Post-Doctoral Fellowship with the Department of Engineering Physics, Polytechnic School of Montreal, Montreal, QC, Canada, and the Materials Chemistry, RWTH Aachen University, Aachen, Germany. In 2007, he was an Associate Professor with the University of Mons, where he is currently a Full Professor and the Head of the Chimie des Interactions Plasma-Surface (ChIPS) Group. Since 2017, he has been a Visiting Professor of the Technical University of Tianjin, Tianjin, China. He is one of the Scientific Director of the Materia Nova Research Center, Mons. He has coauthored more than 180 peer-reviewed papers in thin films synthesis (magnetron sputtering, plasma polymerization,. . .), of plasma functionalization, and of plasma chemistry. He has an H factor of 27. His current research interests include the utilization of low-pressure plasmas for the processing of materials, especially on the characterization of the plasma phase during these processes.

Dr. Snyders is currently the President of the Belgian Vacuum Society (Belvac).

Holger Heuermann (M'06) received the Ph.D. degree in electrical engineering from the University of Bochum, Bochum, Germany, in 1995.

From 1991 to 1995, he was a Research Assistant with the University of Bochum, where he was involved in the field of RF measurement techniques. From 1995 to 1998, he was with Rosenberger Hochfrequenztechnik GmbH & Co. KG, Fridolfing, Germany, where he was engaged in the design of RF equipment for measurements with network analyzers. In 1998, he joined Infineon Technologies, Munich, Germany, where he was leading a development group for wireless front-end modules and integrated circuits. Since 2002, he has been with the Aachen University of Applied Sciences, Aachen, Germany, where he is currently a Professor and the Lead of the Institute for Microwave of Microwave and Plasma Technology (IMP). Since 2008, he has been the Lead of Heuermann HF-Technik GmbH Company, Aachen. He has authored or coauthored more than 90 papers. He holds more than 30 patents. His current research interests include RF components, design of ultra wide-band transceiver circuits, RF plasmas, and high-precision scattering parameter measurements.

Dr. Heuermann was a Long-Term Member of the Microwave Measurements Technical Committee MTT-11.